

exception of the baby boom, which may indeed have been the demographic aberration), and when we see similar and even more extreme declines in other Western countries in recent decades, the conclusion that fertility appears destined to remain low seems inescapable. The greater uncertainty appears to be how low it will fall. The large problems on the demographic horizon in Western countries will be those associated with aging, with population decline, and with questions of immigration.

It is worth remembering that similar prognostications were made in the late 1930's when concerns were expressed about impending population decline in parts of Europe. Events of the next two decades in retrospect made those prognostications look quaint. Quite clearly, there are serious limits to forecasting in the social sciences.

REFERENCES AND NOTES

1. Commission on Population Growth and the American Future, *Population and the American Future* (Government Printing Office, Washington, DC, 1972).
2. National Academy of Sciences, *Immigration Statistics: A Story of Neglect* (Washington, DC, 1985).

3. U.S. Bureau of the Census, *Curr. Popul. Rep. Ser. P-25* (1985), p. 952.
4. R. A. Easterlin, *Birth and Fortune* (Basic Books, New York, 1980).
5. D. R. Vining, Jr., *Popul. Dev. Rev.* **10**, 693 (1984).
6. N. B. Ryder, in *Population and Societal Outlook* (Foundation Roi Baudouin, Brussels, 1984), pp. 269-280.
7. U.S. Bureau of the Census, *Curr. Popul. Rep. Ser. P-20* (1984), p. 389.
8. U.S. Bureau of the Census, *ibid.*, p. 385.
9. D. E. Bloom, "The labor market consequences of delayed childbearing," paper presented at the annual meeting of the American Statistical Association, Chicago, IL, 18 August 1985.
10. N. B. Ryder, unpublished manuscript.
11. C. F. Westoff and N. B. Ryder, *The Contraceptive Revolution* (Princeton Univ. Press, Princeton, NJ, 1977).
12. W. F. Pratt, W. D. Mosher, C. A. Bachrach, M. C. Horn, *Popul. Bull.* **39** (1984).
13. S. K. Henshaw, *Fam. Plann. Perspect.* **18**, 34 (1986).
14. T. Frejka, *ibid.* **17**, 230 (1985).
15. C. F. Westoff, G. Calot, A. D. Foster, *Int. Fam. Plann. Perspect.* **9**, 45 (1983).
16. E. F. Jones *et al.*, *Fam. Plann. Perspect.* **17**, 53 (1985).
17. W. D. Mosher and W. F. Pratt, Vital and Health Statistics, National Center for Health Statistics, *Adv. Data* **104** (1985), p. 1.
18. Alan Guttmacher Institute, "Infertility services in the United States: need, accessibility and utilization" (New York, 1985), unpublished manuscript.
19. C. F. Westoff and E. F. Jones, *Demography* **16** (1978).
20. National Center for Health Statistics, *Mon. Vital Stat. Rep.* **34**, 6 (1986).
21. M. D. R. Evans, *Popul. Dev. Rev.* **12**, 272 (1986).
22. R. W. Gardner, B. Robey, P. C. Smith, *Popul. Bull.* **40** (1985).
23. U.S. Bureau of the Census, *Curr. Popul. Rep. Ser. P-20* (1986), p. 12.

Ablation of Polymers and Biological Tissue by Ultraviolet Lasers

R. SRINIVASAN

When pulsed, ultraviolet laser radiation falls on the surface of an organic polymer or biological tissue, the material at the surface is spontaneously etched away to a depth of 0.1 to several micrometers. In the process, the depth of etching is controlled by the width of the pulse and the fluence of the laser, and there is no detectable thermal damage to the substrate. The material that is removed by etching consists of products ranging from atoms to small fragments of the polymer. They are ejected at supersonic velocities. This dry photoetching technique is useful in patterning polymer films. It is also under serious investigation in several areas in surgery.

A SIMPLE AND CONVENIENT SOURCE OF LASER RADIATION in the ultraviolet (UV) region became available with the invention of the excimer laser in the 1970's. Studies on the interaction of UV laser pulses with solid organic matter such as synthetic polymers and biological tissue led to the discovery in 1982 (1-4) of the phenomenon of "ablative photodecomposition," which results in the breakup of the structure of the organic solid by the photons and the expulsion of the fragments at supersonic velocities. The result is an etch pattern in the solid with a geometry that is defined by the light beam. The principal advantages in using UV laser radiation rather than visible or infrared laser radiation for this

purpose lie in the precision ($\pm 2000 \text{ \AA}$) with which the depth of the cut can be controlled and the lack of thermal damage to the substrate to a microscopic level. The results obtained with a UV laser at 193 nm are compared in Fig. 1 to those with an Nd:YAG (yttrium-aluminum-garnet) laser at 532 nm for etching a sample of human arterial tissue (5).

Mechanism of Absorption of Light

Synthetic organic polymers are made up of molecules which consist of 10^3 to 10^5 atoms, principally carbon, hydrogen, oxygen, and nitrogen. A small molecular unit (monomer) of 6 to 40 atoms is repeated over and over along a chain to form a polymer. In Fig. 2, two typical polymers called poly(methyl methacrylate) (PMMA) and polyimide are shown along with the monomer units in each case. A polymer molecule may consist of 10^2 to 10^3 monomer units. The bonding between atoms within a polymer is covalent (shared electrons) in nature and strong (60 to 150 kcal/mol), but the forces between the molecules are weak (<10 kcal/mol). Absorption of photons of UV wavelength excites the bonding electrons in polymers, and specific absorptions correlate with specific groups of atoms (chromophores) in the molecules. An energy diagram (Fig. 3)

The author is manager of photochemical research at IBM Thomas J. Watson Research Center, Yorktown Heights, NY 10598.

can describe the absorption of a UV photon by one bond A-B in the molecule. The lowest curve represents the lowest (ground) energy state for the bond with the horizontal lines marking vibrational levels within a specific electronic level. Absorption of a UV photon (vertical arrow 1) is such a rapid process that it proceeds with no nuclear motion and leads to an upper electronic level. This is still a bound state as shown here but metastable with respect to the initial state. In the upper state the energy in the bond obviously exceeds the bond energy and therefore the two atoms can dissociate at the very next vibration. But such dissociation processes compete with fluorescence (the reverse of the excitation) and with internal conversion (arrow 2), which results in the crossing of the excited species to its ground-state energy surface with enough energy to dissociate in that state. Since there are numerous other competing processes such as vibrational deactivation, intersystem crossing to a different electronic state, and collisional quenching to take into account, the photophysics and photochemical processes that follow electronic excitation can be complex and difficult to sort out (6).

The details of the interaction of the photon with the electrons in A-B were not specified in the discussion above. Such an interaction can lead to a promotion of a valence electron from a bonding to an antibonding orbital, which is the most common process in the wavelength region >200 nm. With decreasing wavelength, the number of valence excitations increases rapidly and it may not be possible to assign absorptions to specific transitions in a polyatomic molecule. A further complexity becomes evident for wavelengths <200 nm, at which point Rydberg transitions become increasingly important. Rydberg transitions result when an electron from a bonding orbital or an electron from a nonbonding or weakly bonding orbital is promoted to a Rydberg orbital. The convergence limit to the Rydberg transitions is, as in atomic spectroscopy, a (molecular) ion and an electron (7). In polyatomic organic molecules, some or all of these transitions can occur simultaneously.

Structural biological material also consists of polymers, but they are not made up of a single monomer unit. Furthermore, a large component of these materials is water ($\sim 80\%$). Small organic molecules and inorganic ions are also invariably present and contribute to the UV absorption. Compared to the synthetic polymers, it is even more difficult in these systems to sort out the UV absorption and delineate the decomposition pathways.

Laser Ablation Characteristics

Laser pulses from an excimer laser are typically of ~ 20 -nsec half width. A schematic representation of the impact of such a pulse of light on a polymer surface is shown in Fig. 4. The penetration of the radiation through the solid follows a simple relation which is known as Beer's law:

$$I_t = I_0 10^{-\alpha \ell} \quad (1)$$

where I_0 and I_t are the intensities of the beam of light before and after transmission through a slice of material of thickness ℓ , and α , the absorptivity, is a characteristic property of the material. In weak absorbers such as PMMA, a pulse of laser radiation of 193-nm wavelength will penetrate to a 6.5- μm depth before 95% of it would have been absorbed, whereas in a strong absorber such as polyimide, the penetration depth, ℓ_a , will be only a few thousand angstroms. If the fluence F of the laser beam exceeds a certain threshold value, F_0 , then a depth, ℓ_f of the material is ablated by the pulse. At the same time an audible report is heard, and, when the irradiation is carried out in air, a spot of visible light is observed at the point where the laser beam impacts the surface. If the fluence is such that $\ell_f < \ell_a$, which is usually the case, then a depth $\ell_a - \ell_f$ that had been exposed to the light will be left behind. The next pulse will go through this partly irradiated material as well as through virgin material underlying it. The first pulse is therefore unique. But after the first few pulses, there is a linear relation between the number of pulses and the depth that is etched. In practice, the depths etched by varying numbers of pulses are averaged and noted as the etch depth per pulse for that polymer at that wavelength and fluence. This value is reproducible within the uncertainty ($\pm 8\%$) in the measurement of the etch depth and the fluence of the laser pulse. This is the reason that the etch depth can be reproduced to ± 2000 Å in most materials.

A typical plot of the etch depth per pulse as a function of fluence is shown in Fig. 5 for polyimide. The three wavelengths shown correspond to the strong output lines of the excimer laser depending on the gas fill. The etch depth is independent of the atmosphere in which the experiment is performed, which is one of the attractive features of this process. The threshold fluence for the onset of etching decreases with decreasing wavelength. But, in general,

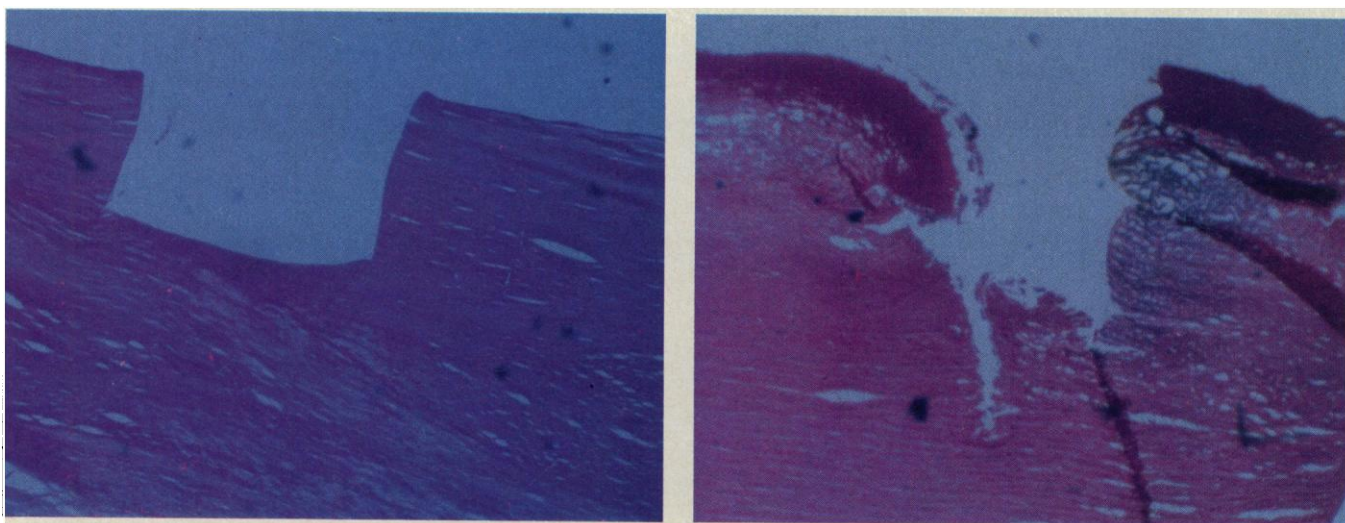


Fig. 1. Cross section of luminal side of an aortic wall [reproduced from (5) with permission of Liss]. (Left) Trench (0.35 mm) produced by laser radiation at 193 nm; pulse duration, 14 nsec; fluence, 0.25 J/cm^2 . (Right) Crater (0.4 mm) produced by laser radiation at 532 nm; pulse duration, 5

nsec; fluence, 1.0 J/cm^2 . The absorption coefficients of the material at the two wavelengths are vastly ($\sim 10^3$) different. This would lead to a considerable difference in the energy deposited per unit volume of ablated material.

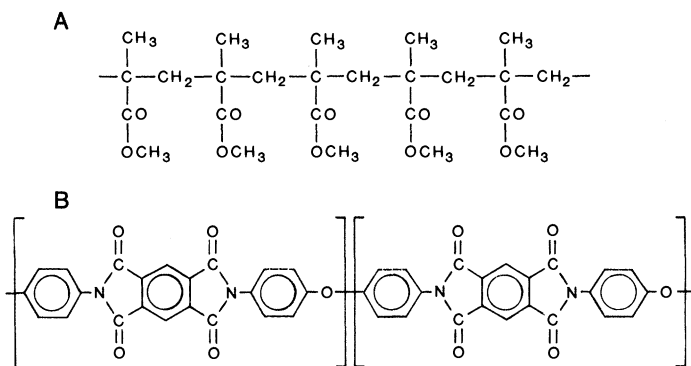


Fig. 2. Formulas of two synthetic polymers: (A) poly(methyl methacrylate) (PMMA) and (B) polyimide (DuPont Kapton).

amount of material removed (that is, the etch depth per pulse) increases with increasing wavelength and fluence. Fluence thresholds for etching and etch depth plots for a variety of synthetic polymers as well as for cornea, arterial wall, and skin have been reported (2, 3, 8-16).

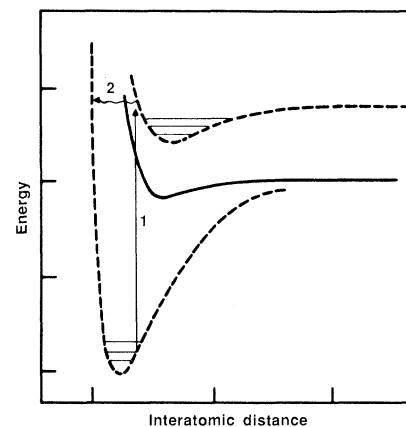
In one study (17), the thresholds and etch rates in PMMA at 90 K and 273 K were compared. At a laser wavelength of 193 nm, there was no difference in the etching characteristics at the two temperatures. At 248 nm, however, the etch rate at a given fluence at 90 K was only half of the value at 273 K. The thresholds remained unaffected.

The products of UV laser ablation have been analyzed in a few polymers (1, 9, 18-20). In every instance there appears to be a diversity of products ranging from atoms and diatomics to small polyatomic molecules and small fragments of the polymer. The product composition is also wavelength-dependent. From PMMA of initial number-average molecular weight (M_n) = 10^6 , at 193 nm, the products are oxides of carbon, MMA (the monomer) and low molecular weight ($M_n < 1500$) fragments of the polymer. At 248 nm, the principal product is a low molecular weight fraction ($M_n = 2500$) of the polymer. From polyimide, the products are oxides of carbon, benzene, hydrocyanic acid (HCN), and elemental carbon. In addition to these stable products, transient intermediates such as C_2 , CN, CH, and C have also been detected in the same systems by means of fast methods of analysis described below. Reference has already been made to the depth $\ell_a - \ell_f$ under the etched surface, which is transformed by the laser photons but is left behind in the substrate. This freshly created surface has been analyzed by x-ray photoelectron spectroscopy (XPS) and by wet chemical methods (21). In oxygen-containing polymers such as polyimide, this surface is found to be depleted in oxygen, and the change is attributed to the loss of oxides of carbon. The penetration depth for XPS analysis is ~ 100 Å. Since the etched surface of a polymer can be irregular to the extent of several hundred angstroms, it has not been established to what depth this chemical change actually extends. Wet reactions show that there may even be a very thin (< 50 Å) layer that has undergone oxidation by air on top of the altered layer that is seen by XPS.

Low molecular weight products (C_1 to C_4) from the laser ablation in vitro of human arterial tissue have been analyzed (13), but it is not clear if solid high molecular weight products are also ablated in this instance. The deposition of solid debris has been reported at the edge of cuts made in vivo by 193-nm laser pulses in rabbit cornea (22). Changes in the ultrastructure of corneal tissue adjoining or underlying an ablated cut have been carefully studied (22).

The dynamics of the ejection of the material during the etching of a polymer by a laser pulse has been studied in several ways. Even at

Fig. 3. Energy-level diagram for hypothetical bond A-B. The lower broken line represents the ground electronic state; the upper broken line and the solid line represent excited electronic states.



fluence levels below the threshold for etching of PMMA or polyimide, the ejection of diatomic species such as C_2 and CN at peak velocities as large as 6×10^5 to 7×10^5 cm/sec can be observed by laser-induced fluorescence (LIF) (19, 23). The peak velocity changed by less than 20% over a 14-fold increase in fluence (0.05 to 0.70 J/cm²; 248 nm), which caused a several hundred-fold increase in the amplitude of the signal. The corresponding translational temperature would be many tens of thousands of degrees. An analysis of the rotational spectrum of the fluorescence indicated that the rotational temperature was only 1000 ± 200 K. As the fluence is

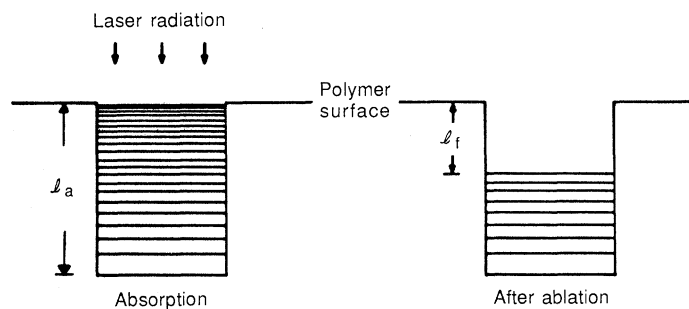


Fig. 4. Schematic representation of impact of laser pulse on polymer surface.

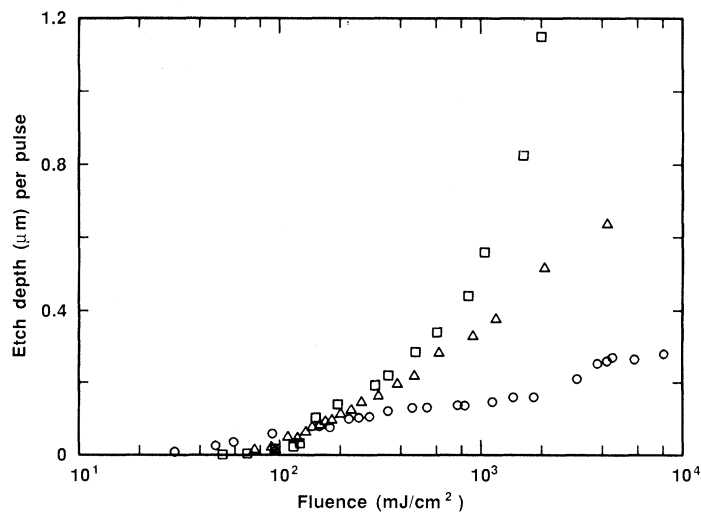
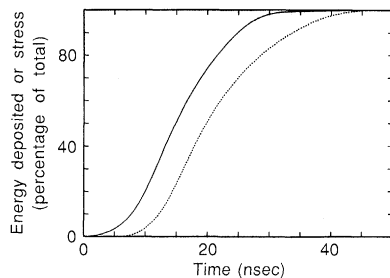


Fig. 5. A plot of depth of material removed per pulse as a function of fluence; sample: polyimide film, $125 \mu\text{m}$ thick. Laser pulse: \circ , 193 nm; \triangle , 248 nm; \square , 308 nm. Each data point averaged more than ten to several hundred pulses; uncertainty, $\pm 8\%$.

Fig. 6. Plots of the fraction of energy deposited in one pulse and fraction of integrated amplitude of stress pulse as a function of time. Solid line, energy; dashed line, stress pulse; sample, polyimide film, 7.5 μm thick; 193-nm laser pulse. Data from photoacoustic measurement (27).



progressively increased, these species are observed in emission (24). Atoms (C) and ions (C⁺) are also seen. CH has been observed in emission from PMMA at 193 nm. An analysis of its spectrum showed that its vibrational and rotational temperatures are both equal to 3200 ± 200 K (25). The translational temperature was estimated by timing its velocity to be $\sim 11,000$ K. The velocity of the polyatomic product MMA formed in the laser ablation of PMMA at 193 nm was measured by time-of-flight mass spectrometry (26). At fluences < 0.12 J/cm², which are near the threshold for ablation, the translational temperatures ranged from 1000 to 3000 K. There is thus a difference in the translational temperatures between a polyatomic product and a transient diatomic product from the same polymer, which suggests that they may be formed by different reaction paths.

The temporal profile of ablation was determined by a photoacoustic measurement of the stress wave induced in a polymer film by the ejection of the ablating material (27). A thin, piezoelectric transducer attached to the polymer film timed the stress wave with an uncertainty of ± 1 nsec. The delay due to travel of the stress wave through the film was compensated. Below the threshold for ablation, a pulse of UV radiation merely heats the polymer sample (16, 28) and gives rise to a sinusoidal stress pulse. But above the threshold, a strong positive signal is obtained that increases rapidly

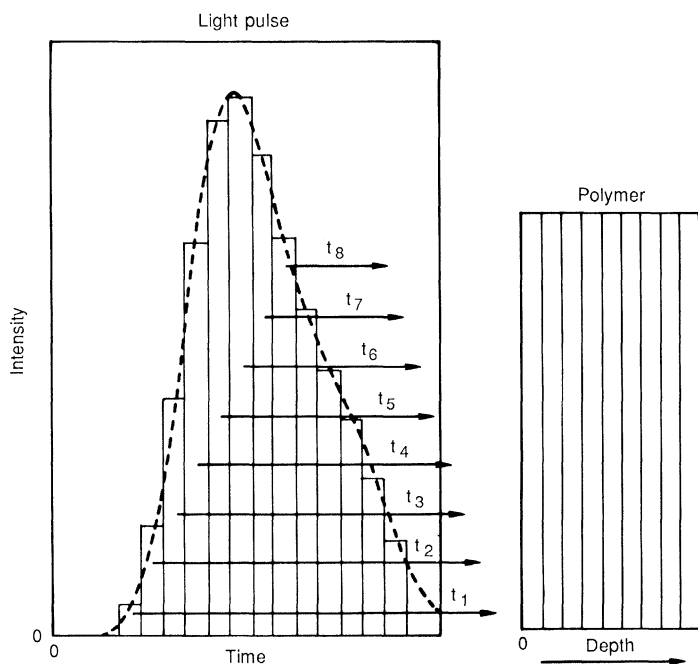


Fig. 7. Schematic of interaction of a single laser pulse with a polymer sample. Successive slices (in time) of the light pulse are shown to be absorbed in hypothetical layers of the material according to Beer's law. When the concentration of absorbed photons in any one layer exceeds an ablation threshold, that layer will ablate.

with increasing fluence. The temporal delay between the onset of the laser pulse and the onset of ablation is 7 nsec, which is well within the half width of the laser pulse. This behavior is common to PMMA, polyimide, and rabbit cornea even though these materials differ widely in their absorption characteristics and chemical composition.

The "doping" of a polymer to change its UV absorption and thereby increase its sensitivity to UV laser ablation shows interesting potential. In one investigation (29), it was found that the introduction of acridine, a small molecule ($M_r = 179$), in concentrations of 1 to 8% by weight in PMMA progressively reduced the threshold for ablation at 248 nm and also sensitized it to laser etching at 308 nm. Undoped PMMA is transparent to radiation of 308-nm wavelength.

Mechanism of UV Ablation

The mechanism by which UV laser pulses bring about the etching of polymer surfaces with a minimum of thermal damage to the substrate has been a matter of controversy. Two aspects to this problem are: (i) the reaction path in which the polymer bonds are actually broken, and (ii) a quantitative model of etch behavior as a function of pulse width, wavelength, and fluence.

The principal reaction paths that have been proposed can be understood by referring to the energy diagram in Fig. 3. It is generally accepted that the absorption of UV photons results in electronic excitation (path 1). The excited electronic state can undergo decomposition in that state, which would be a purely photochemical reaction; or, if the excited molecule undergoes internal conversion (path 2) to a vibrationally excited ground state, any subsequent decomposition can be considered to be the equivalent of a thermal process. This is the so-called photothermal mechanism in which the photons merely act as a source of thermal energy. Along either pathway the products can be the same (although they do not have to be) and any excess energy over that needed to break the bonds will remain in the products and will be dissipated in the ablated fragments. If the time for ablation is of the order of the duration of the laser pulse (~ 20 nsec), the diffusion of the thermal energy to the substrate would be minimal [a diffusion length of a few hundred angstroms has been estimated (9)] and therefore it would be expected that the substrate would experience no thermal damage (9, 28).

The expression

$$\ell_f = \frac{1}{\alpha} \log \frac{F}{F_0} \quad (2)$$

which relates the etch depth per pulse to the fluence, the fluence threshold, and the absorptivity at that wavelength, has been derived by more than one group of workers (2, 3, 8, 9, 30). The derivation merely relates to the deposition of the photon energy according to Beer's law (Eq. 1) and is independent of the assumed mechanism. The test of Eq. 2 lies in whether a plot of ℓ_f versus $\log F$ is a straight line with a slope equal to $1/\alpha$. The linear relation is certainly not true for polyimide (Fig. 5) but earlier work in which data were obtained over a smaller range of fluences allowed a linear relation to be forced through the experimental points. The slope of such plots was invariably not equal to $1/\alpha$.

Early views of this phenomenon implicitly assumed that ablation followed the deposition of all of the photons of the laser pulse in the solid. But the photoacoustic experiments mentioned in the previous section typically showed (Fig. 6) that, when a small fraction of the pulse energy had been deposited in the film, the material started to ablate. In these experiments, it was established that the onset of the photoacoustic pulse actually coincided with the onset of ablation.

This temporal behavior of the system is also consistent with a simulation of UV laser ablation that has been carried out (31) in which, if it was assumed that at time $t = 0$ the photons were already absorbed in the first several layers of the material and the polymer bonds were broken, then the monomer ablated layer by layer, and the first layer was free from the surface in <3 psec.

A knowledge of the time profile of ablation affects the interpretation of the calculations of the temperature rise in the volume of material that ablated. These calculations, which form the basis for the photothermal mechanism, significantly overestimated the temperature. It can be shown that the actual rate of thermal decomposition would not be adequate to lead to ablation in the time span of the laser pulse. For example, the data on polyimide (Fig. 6) show that material begins to ablate in <10 nsec and at that point, based on the amount of energy absorbed, the temperature rise would be 1200 K in the absorption depth (95%) of $0.07 \mu\text{m}$. However, the half-life for the thermal decomposition of a polyimide at this temperature has been measured to be ~ 20 seconds (32). It can be argued that the rate constants to be used to estimate thermal decomposition half-lives under pulsed laser irradiation conditions are not those obtained from slow pyrolysis studies in static systems. The discordance between the two sets of data is so enormous ($\sim 10^9$) that it is hard to believe that they can be reconciled. Such discordance between laser ablation and pyrolysis data is observable at other wavelengths for polyimide (19). An analysis for PMMA that leads to similar conclusions has been reported (18).

A realistic model of the interaction of UV laser pulses with an organic solid has been proposed (33), which takes into account that as the photons penetrated the material and bonds were broken, the photon intensity at any depth ℓ will evolve with time:

$$I(\ell, t) = I_0(t) \exp[-k' \int_0^\ell d\ell' n(\ell', t)] \quad (3)$$

where I_0 is referred to as the unshielded laser intensity, k is a constant, and n is the density of unbroken polymer bonds. If n is not a function of time, this expression will reduce to Beer's law. The change in n with time is given by

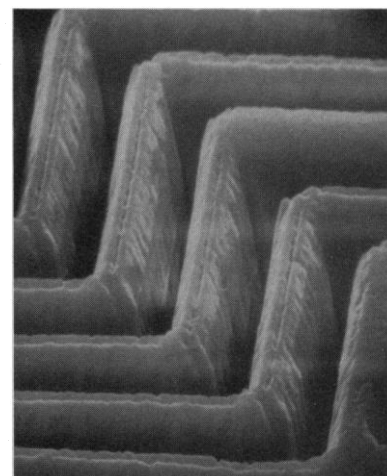
$$n(\ell, t) = -kI(\ell, t) n(\ell, t) \quad (4)$$

When Eq. 3 is substituted into Eq. 4 and solved for the initial condition $n(\ell, t = 0) = 0$ when $\ell < 0$; $n(\ell, t = 0) = n_\infty$ when $\ell > 0$, then

$$\frac{n(\ell, t)}{n_\infty} = \{1 + [\exp(kI_0 t) - 1] \exp(-k'n_\infty \ell)\}^{-1} \quad (5)$$

The time-dependent passage of the laser pulse through the ablating material that is explained in this theory has been adapted in a more recent approach (34), which is tailored to the practical question of relating the etching behavior to experimental parameters. A photochemical mechanism is assumed here, and the rate of decomposition of the polymer in its excited state is viewed as a process that competes with alternative processes for the degradation of the energy, alternatives that do not lead to decomposition. The width of the laser pulse is a critical factor, because it is only the flux of absorbed photons above a threshold value that will be available for bond-breaking. The laser pulse is considered to be made up of a continuous succession of short (~ 20 -psec) pulses whose passage through the solid is followed by its absorption in successive layers of the material (Fig. 7). The deposition of photon energy in each layer can be calculated from Beer's law. The ablation condition is met when the number of absorbed photons in a given volume exceeds a certain value. It is necessary to determine the ablation condition from the experimental data at one wavelength, which simultaneously gives the threshold level of the absorbed photon flux. The model

Fig. 8. Sample of photoresist film patterned by 193-nm laser pulses. Sample: polyacrylate material (DuPont Riston); lines shown are $5 \mu\text{m}$ thick. [Scanning electron microphotograph by K. Brown]



can then be applied to UV etching at other wavelengths for the same polymer without further adjustment of any parameter. The predictions made from this model regarding the relation between the pulse width and fluence thresholds (a factor of importance in practical applications) are being tested and have yielded encouraging results.

In summary, at present there is little evidence to support a purely photothermal mechanism for the UV laser ablation of any polymer. A photochemical mechanism is more probable, but it may be much more complex in nature than originally proposed (8). The process of excitation may include not only the first upper excited electronic state but, through multiphoton processes, higher states as well. Thermal activation of photochemical decomposition is another consideration in the near-UV wavelengths.

Technological Applications

A reliable excimer laser that can be built into an industrial tool is a prerequisite if UV laser ablation is to make an impact as a technology. When the first commercial excimer lasers became available at the end of the 1970's, they were little more than research instruments. The developments that have taken place in the intervening years have led to the offering of the first industrial model by the mid 1980's, which is a sure indication of the promise for the future that exists in this laser. Currently several models of excimer lasers that will deliver a constant ($\pm 10\%$) preset output of energy are available from different manufacturers. These machines are internally controlled by a microprocessor and are said to be good for several tens of millions of pulses before any serious maintenance will be needed (35).

The most obvious application of UV laser etching may seem to be in photolithography (36). This is the process that is used widely in semiconductor processing to pattern silicon, oxide, or metal surfaces by a procedure analogous to photography. A light-sensitive organic polymer film called a "photoresist" acts as the medium for the patterning. In present practice, after exposure to a light source that registers a pattern, the photoresist is developed by wet chemical methods. It has been demonstrated (Fig. 8) that photoresists can be patterned by means of proximity printing (37) or projection printing with UV laser radiation. Resolution extending down to $0.3 \mu\text{m}$ has been claimed. Another feature of this technique that can be exploited is the high aspect ratio (up to 20:1) that is attainable with wall angles overcut 1° to 30° off the vertical. However, photolithography with existing wet methods is so highly developed that it will be many years before this dry etching process will become competitive.

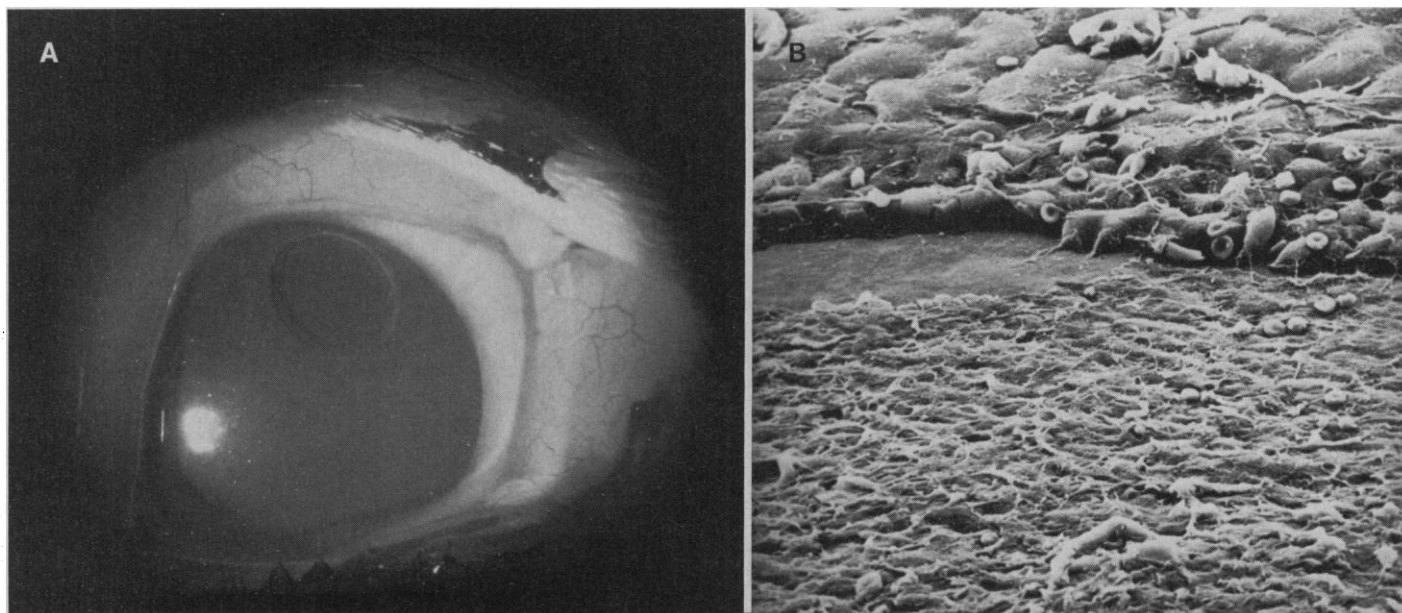


Fig. 9. (A) Cornea of rabbit. A circular disk pattern was etched by 193-nm laser pulses. It demonstrates the capability of this technique to remove organic material over several square millimeters of tissue with considerable degree of control over the depth so that a relatively smooth surface is left

behind. (B) Scanning electron microphotograph of cornea at left showing the smoothness of the etched surface. The scale is shown by the red corpuscles (diameter, 5 μm) in view. [Photographs by S. L. Trokel and J. Marshall]

The attractive applications at present are those in which UV laser ablation offers unique possibilities. For example, the class of polymers called polyimides, one of which is represented in Fig. 2B, are important industrially because of their toughness and electrical properties. But their resistance to chemicals and heat make them difficult to pattern by any conventional method (38). The only procedure by which a polyimide film could be geometrically altered was by patterning a precursor material that could subsequently be chemically converted to the final polyimide structure. Now, UV laser etching offers a convenient solution to the problem (9, 20, 38). An important advantage of UV laser (in contrast to an infrared laser) is in the lack of carbonization at the new surfaces that are created, because a surface film of carbon alters the electrical properties of the film in an undesirable way.

The economics of the polymer industry is such that an expensive technique such as UV laser ablation would benefit only a specialty polymer as a part of a highly valued product. Such opportunities may be expected to develop gradually in optics, electronics, and aerospace industries.

Surgical Applications

Before the advent of the excimer laser, lasers for surgery usually have been used for controlled burning and removal of tissue based on the thermal effects of visible and infrared radiation (39). A significant exception was the use of laser-induced optical breakdown to section tissues inside the eye by the formation of a plasma and the associated shock waves (40). The excimer laser offers a third kind of laser-tissue interaction, which, as already exemplified, results in the ablation of the tissue without thermal damage to the adjacent structures that remain behind.

The use of UV laser ablation in surgery requires several considerations that are not critical in technological applications. These are the problem of delivering the photons to an irradiation site inside the body, the control of the exposure to limit the cutting to a defined area and to a required depth, the course of healing of the tissue after exposure, and the potential for mutagenesis caused by

the photons. A number of investigations have been reported that deal with the potential use of UV lasers in surgery on the cornea (11, 22, 41), on the skin (15), in angioplasty (5, 12-14, 42, 43), and in neurosurgery (44). It is not possible here to discuss all of these studies in detail, but mention will be made of the present state of development in two of the areas that have attracted the most activity.

The excimer wavelength of 193 nm has been found to be particularly suitable for surgery on the cornea since the morphology of the cut is superior to those obtained when radiation at other wavelengths in the UV (for example, 248 nm) or infrared is used (22). Furthermore, the high absorption cross section for this wavelength limits the depth of the damage at the bottom and sides of the cut, and mutagenesis is also minimal or nonexistent. The possibility of not only creating grooves but of reshaping an entire surface to generate a controlled refractive path in the cornea (Fig. 9) has aroused much interest.

The use of UV wavelengths for laser angioplasty has also attracted considerable research interest, but its status is clouded in controversy. The first problems are the obvious ones of delivery of the radiation via catheters to the site and the removal of the products by suction. The fiber optics needed for this purpose are still in development. The use of UV wavelengths is itself in competition with the use of visible wavelengths, also from a laser, for the same purpose, presumably by a thermal decomposition mechanism. Whether UV laser angioplasty will work on calcified plaque or not is also under debate. A successful process that overcomes these problems would have such widespread benefits to humanity that active research in this area will undoubtedly continue.

Conclusion

UV laser ablation of organic matter promises to be of continuing interest as research extends into the physics and chemistry of the process in greater detail. Its importance to technology and medicine will grow with increasing availability of dependable lasers and sophisticated delivery systems.

REFERENCES AND NOTES

1. R. Srinivasan and V. Mayne-Banton, *Appl. Phys. Lett.* **41**, 576 (1982); R. Srinivasan and W. J. Leigh, *J. Am. Chem. Soc.* **104**, 6784 (1982).
2. M. W. Geis *et al.*, *Appl. Phys. Lett.* **43**, 74 (1983); T. F. Deutsch and M. W. Geis, *J. Appl. Phys.* **54**, 7201 (1983).
3. J. E. Andrew, P. E. Dyer, D. Forster, P. H. Key, *Appl. Phys. Lett.* **43**, 717 (1983).
4. M. Murahara, Y. Kawamura, K. Toyoda, S. Namba, *Obyo Butsuri* **52**, 83 (1983).
5. R. Linsker, R. Srinivasan, J. J. Wynne, D. R. Alonso, *Lasers Surg. Med.* **4**, 201 (1984).
6. J. G. Calvert and J. N. Pitts, Jr., *Photochemistry* (Wiley, New York, 1966).
7. M. B. Robin, *Higher Excited States of Polyatomic Molecules* (Academic Press, New York, 1974).
8. R. Srinivasan, *J. Vac. Sci. Technol. B* **4**, 923 (1983); ——— and B. Braren, *J. Polym. Sci. Polym. Chem. Ed.* **22**, 2601 (1984).
9. J. H. Brannon, J. R. Lankard, A. I. Baise, F. Burns, J. Kaufman, *J. Appl. Phys.* **58**, 2036 (1985).
10. H. S. Cole, Y. S. Liu, H. R. Philipp, *Appl. Phys. Lett.* **48**, 76 (1986).
11. S. L. Trokel, R. Srinivasan, B. Braren, *Am. J. Ophthalmol.* **96**, 710 (1983); R. Krueger and S. L. Trokel, *Arch. Ophthalmol.* **103**, 1741 (1985).
12. T. J. Bowker *et al.*, *Lasers Med. Sci.*, in press.
13. D. L. Singleton *et al.*, *Appl. Phys. Lett.* **48**, 878 (1986).
14. W. S. Grundfest *et al.*, *J. Am. Coll. Cardiol.* **5**, 929 (1985).
15. R. J. Lane, R. Linsker, J. J. Wynne, A. Torres, R. G. Geronemus, *Arch. Dermatol.* **121**, 609 (1985).
16. P. E. Dyer and J. Sidhu, *J. Appl. Phys.* **57**, 1420 (1985).
17. B. Braren and D. Seeger, *J. Polym. Sci. Polym. Lett. Ed.*, in press.
18. R. Srinivasan *et al.*, *Macromolecules* **19**, 916 (1986).
19. R. Srinivasan, B. Braren, R. W. Dreyfus, *J. Appl. Phys.*, in press.
20. J. T. C. Yeh, *J. Vac. Sci. Technol. A* **4**, 653 (1986).
21. S. Lazare, P. D. Hoh, J. M. Baker, R. Srinivasan, *J. Am. Chem. Soc.* **106**, 4288 (1984); S. Lazare and R. Srinivasan, *J. Phys. Chem.* **90**, 2124 (1986).
22. J. Marshall, S. Trokel, S. Rothery, H. Schubert, *Ophthalmology* **92**, 749 (1985); J. Marshall, S. Trokel, S. Rothery, R. R. Krueger, *Br. J. Ophthalmol.* **70**, 482 (1986).
23. R. Srinivasan and R. W. Dreyfus, *Springer Ser. Opt. Sci.* **49**, 396 (1985).
24. G. Koren and J. T. C. Yeh, *Appl. Phys. Lett.* **44**, 1112 (1984); *J. Appl. Phys.* **56**, 2120 (1984).
25. G. M. Davis, M. C. Gower, C. Fotakis, T. Efthimiopoulos, P. Argyrakis, *Appl. Phys. A* **36**, 27 (1985).
26. B. Danielzik, N. Fabricius, M. Rowekamp, D. von der Linde, *Appl. Phys. Lett.* **48**, 212 (1986).
27. P. E. Dyer and R. Srinivasan, *ibid.* **48**, 445 (1986).
28. G. Gorodetsky, T. G. Kazyaka, R. L. Melcher, R. Srinivasan, *ibid.* **46**, 828 (1985).
29. R. Srinivasan, B. Braren, L. Hadel, R. W. Dreyfus, D. Seeger, *J. Opt. Soc. B* **3**, 785 (1986).
30. H. H. G. Jellinek and R. Srinivasan, *J. Phys. Chem.* **88**, 3048 (1984).
31. B. J. Garrison and R. Srinivasan, *Appl. Phys. Lett.* **44**, 849 (1984); *J. Appl. Phys.* **57**, 2909 (1985).
32. H. H. G. Jellinek and S. R. Dunkle, *J. Polym. Sci. Polym. Chem. Ed.* **21**, 2111 (1983). The polyimide used in this study differs from the structure shown in Fig. 2B in having a methylene bridge instead of an ether bridge.
33. T. Keyes, R. H. Clarke, J. M. Isner, *J. Phys. Chem.* **89**, 4194 (1986).
34. E. Sutcliffe and R. Srinivasan, *J. Appl. Phys.*, in press.
35. H. Pummer, U. Sowada, P. Oesterlin, U. Rebhan, D. Basting, *Laser Optoelektron.* **17**, 141 (1985).
36. S. E. Blum, K. H. Brown, R. Srinivasan, U.S. Patent 4 414 059 (1983).
37. S. Rice and K. Jain, *Appl. Phys. A* **33**, 195 (1984).
38. J. H. Brannon, J. R. Lankard, A. I. Baise, F. Burns, J. Kaufman, U.S. Patent 4 508 749 (1983).
39. V. S. Letokhov, *Nature (London)* **316**, 325 (1985).
40. S. L. Trokel, *YAG Laser Ophthalmic Microsurgery* (Appleton-Century-Crofts, East Norwalk, CT, 1983).
41. C. A. Puliafito *et al.*, *Ophthalmology* **92**, 741 (1985).
42. J. M. Isner and R. H. Clarke, *IEEE J. Quantum Electron.* **QE20**, 1471 (1981); J. M. Isner *et al.*, *Circulation* **68**, 5 (1984).
43. J. J. Haller, M. H. Wholley, E. R. Fisher, E. M. Krokosky, R. Srinivasan, *Cardio* **2**, 31 (1985).
44. H. Normes, R. Srinivasan, R. Solanki, E. Johnson, *Soc. Neurosci.* **11**, 1167 (1985).
45. I thank B. Braren for her assistance in the preparation of this manuscript.

